Korean J. Chem. Eng., 38(11), 2286-2293 (2021)
DOI: 10.1007/s11814-021-0852-y

pISSN: 0256-1115
eISSN: 1975-7220

Ultrasonic cavitation bubble- and gas bubble-assisted adsorption of paclitaxel from *Taxus chinensis* onto Sylopute

Da-Yeon Kang and Jin-Hyun Kim†

Department of Chemical Engineering, Kongju National University, Cheonan 31080, Korea
(*Received 15 March 2021 • Revised 13 May 2021 • Accepted 18 May 2021*)

Abstract−This study presents a technique for adsorption of paclitaxel on Sylopute using ultrasonic cavitation bubbles and gas bubbles. Compared with the conventional adsorption (control), the adsorbed amount and adsorption rate constant increased, respectively, by 1.27-1.44 times and 7.44-9.71 times in ultrasonic adsorption (with mixing at 80-250 W), 1.14-1.27 times and 4.63-9.31 times in ultrasonic adsorption (without mixing at 80-250 W), and 1.06-1.19 times and 1.18-1.34 times in gas bubble-adsorption (without mixing at 1.15-9.41 L/min). As a result of investigating the adsorption mechanism in which cavitation bubbles were introduced, it was shown that microjets and shock waves produced by bubble collapse, rather than the bubble itself, drastically improve mass transport in the pores of the adsorbent, thereby completely eliminating intraparticle diffusion resistance. In the case of gas bubbles, although the intraparticle diffusion coefficient increased by 1.34-1.75 times compared with the control, there was a limitation in promoting intraparticle diffusion.

Keywords: Paclitaxel, Adsorption, Ultrasonic Cavitation Bubble, Gas Bubble, Mechanism

INTRODUCTION

Paclitaxel is a hydrophobic tubulin-binding diterpenoid anticarcinogen found in the bark of yew trees [1]. It is widely used in the treatment of metastatic ovarian cancer, breast cancer, Kaposi's sarcoma, and lung cancer [2]. Paclitaxel is mainly produced by direct extraction from the yew tree [3], semi-synthesis using precursors (baccatin III, 10-deacetylbaccatin III, 10-deacetylpaclitaxel, etc.) [4], and plant cell culture using callus induced from leaf explants of yew trees [5,6]. Among them, extraction and semi-synthesis have difficulties in mass production of paclitaxel from the viewpoint of raw material supply, isolation and purification, recovery rate, and environmental protection. However, plant cell culture can stably mass-produce paclitaxel of uniform quality in a bioreactor without being limited by climate or environment [7].

The isolation and purification process of paclitaxel from plant cells (biomass) generally consists of biomass extraction with an organic solvent, liquid-liquid extraction, adsorption, hexane precipitation, fractional precipitation, and chromatography [6]. Among them, adsorption is well-established in terms of process efficiency, flexibility, and feasibility; it can efficiently remove not only biomass-derived tar and waxy compounds, but also paclitaxel precursors [8]. As typical commercial adsorbents, Sylopute, activated carbon, and active clay can be used, among which Sylopute is excellent in terms of the recovery rate of paclitaxel and the filtration rate after adsorption [8,9].

Recently, various studies have been conducted to improve adsorption efficiency by introducing ultrasonic waves into the adsorption process [10-13]. The improvement in adsorption efficiency is based on acoustic cavitation phenomena including formation, growth, and collapse of microbubbles in a liquid irradiated with ultrasonic waves. That is, the cavitation bubble formed by ultrasonic waves eventually collapses, resulting in high-speed microjets of solution, intense localized heating, and high-pressure shock waves [12]. However, the mechanism of ultrasonic adsorption is still not clear. Furthermore, no investigation has been undertaken on the adsorption mechanism of paclitaxel using ultrasonic waves. Therefore, in this study, ultrasonic cavitation bubbles and gas bubbles were introduced in the adsorption process of paclitaxel derived from *Taxus chinensis* to investigate in more detail the ultrasonic adsorption mechanism. Whereas ultrasonic cavitation bubbles first expand and then collapse, gas bubbles only expand during their lifetime so that no high temperatures or pressures occur. If the bubble plays a central role in adsorption, gas bubbles as well as cavitation bubbles should induce similar adsorption efficiency. In consideration of these characteristics, this study examined the adsorption behavior of paclitaxel and clarified the adsorption mechanism accordingly. In addition, the effect of gas bubbles instead of ultrasonic cavitation bubbles on adsorption efficiency was investigated. Adsorption characteristics were quantitatively identified through kinetics and mechanism analysis. Ultimately, by presenting a new adsorption method incorporating ultrasonic cavitation bubbles and gas bubbles, we attempted to dramatically improve the adsorption efficiency.

MATERIALS AND METHODS

1. Preparation of Paclitaxel Sample

Paclitaxel used in this experiment was obtained by suspension culture (24 °C, 150 rpm, darkness condition) of a cell line derived from the leaves of *Taxus chinensis* [14]. After plant cell cultivation, plant cells (biomass) were collected from the culture broth using a

†To whom correspondence should be addressed.
E-mail: jinhyun@kongju.ac.kr

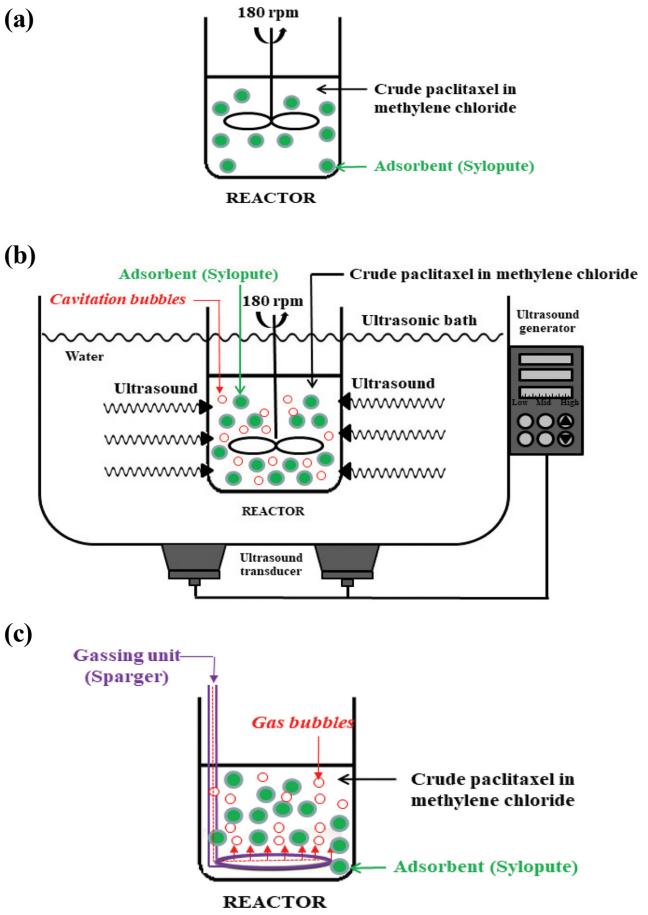

Fig. 1. Schematic diagram of conventional adsorption (a), ultrasonic cavitation bubble-adsorption (b), and gas bubble-adsorption (c) of paclitaxel.

decanter (Westfalia, CA150 Clarifying Decanter) and a high-speed centrifuge (α-Laval, BTPX205GD-35CDEEP). The paclitaxel sample (purity: 90%) for the adsorption process was obtained from plant cells by biomass extraction with methanol, liquid-liquid extraction with methylene chloride, hexane precipitation, fractional precipitation, and silica- and C18-liquid chromatography [15].

2. Adsorption Process

A schematic diagram of conventional adsorption and adsorption using ultrasonic cavitation bubbles and gas bubbles is shown in Fig. 1. Conventional adsorption (control) was performed in a glass reactor under agitation (180 rpm) at 25 °C after first dissolving a sample in methylene chloride (6,500 mg/L) and adding an adsorbent Sylopute (10 g/L). Samples were collected and analyzed at 1, 3, 5, 7, and 10 min of adsorption, respectively. Ultrasonic cavitation bubble-adsorption was performed by irradiating ultrasonic waves (power: 80, 180, 250 W) through a 40 kHz ultrasonic bath (UC-10, Jeiotech, Korea) under the same conditions (temp.: 25 °C, agitation speed: 150 rpm) as the control group. In addition, the same experiment was performed without stirring to investigate the effect of mixing in the adsorption process. Samples were collected and analyzed at 1, 4, 7, and 10 min of adsorption, respectively. Gas bubble-adsorption was performed by introducing gas (gas flow rate: 1.15, 4.52, 9.41 L/min) through a gassing unit (SH-A2, Amazonpet, Korea) equipped with orifices (diameter: 0.5 mm) under the same conditions (except mixing) as the control group. Furthermore, the effect of cavitation bubbles was studied by degassing the adsorption solution, thereby removing dissolved air. The solvent (methylene chloride) used for adsorption was placed in a 40 kHz ultrasonic cleaner, and then degassed by vacuuming for 4 h using an aspirator (A-3S, Tokyo Rikakikai Co., Japan). Thereafter, ultrasonic adsorption (ultrasonic power: 250 W) without mixing was performed using the degassed solution. Whereas cavitation bubbles eventually become unstable and implode during compression and expansion, gas bubbles only expand (no collapse) and do not generate high temperature or pressure. Using these characteristics, the mechanism of ultrasonic adsorption was investigated in detail. Samples were collected and analyzed at 1, 4, 7, 10, and 15 min of adsorption, respectively. The main component, pore volume, surface area, and pore diameter of Sylopute (synthetic silica gel) were SiO_2, 1.81 cm^3/g, 331 m^2/g, and 40-60 nm, respectively. The filtrate obtained by filtration after adsorption was dried in a vacuum oven (UP-2000, EYELA, Japan) at 40 °C for 24 h, and then the adsorbed amount of paclitaxel was analyzed using HPLC. The adsorbed amount in accordance with the adsorption time was calculated using Eq. (1) [16].

$$q_t = (C_0 - C_t)\frac{V}{W} \tag{1}$$

where C_0 and C_t (mg/L) are the concentration of paclitaxel at initial and any time t, respectively, V (L) is the solution volume, and W (g) represents the mass of Sylopute used.

The following equations were used to analyze the adsorption kinetics and mechanism and to verify the validity of the kinetic models.

2-1. Pseudo-second-order Model

The pseudo-second-order kinetic model is expressed as Eq. (2) [17].

$$\frac{t}{q_t} = \frac{1}{k_2 q_e^2} + \frac{1}{q_e}t \tag{2}$$

where q_t and q_e (mg/g) are the amount of paclitaxel adsorbed per unit mass of adsorbent at time t and the amount of paclitaxel adsorbed per unit mass of adsorbent at equilibrium, respectively, and k_2 (g/mg·min) is the pseudo-second-order rate constant.

2-2. Intraparticle Diffusion Model

The intraparticle diffusion model was applied to determine the intraparticle diffusion mechanism including the rate-determining step [18]. The empirical formula shows, as in Eq. (3), that the adsorption capacity is proportional to $t^{1/2}$.

$$q_t = k_p t^{1/2} + C \tag{3}$$

where k_p (mg/g·$min^{1/2}$) is the intraparticle diffusion rate constant.

2-3. Estimation of the Intraparticle Diffusion Coefficient

In the case where intraparticle diffusion is a rate-limiting step, that is, when the adsorption rate is controlled by intraparticle diffusion, the intraparticle diffusion coefficient can be calculated from Eq. (4) [19].

$$-\log\left[1-\left(\frac{q}{q_e}\right)^2\right] = \frac{4\pi^2 D}{2.3d^2}t \tag{4}$$

where q and q_e (mg/g) are the adsorbed amount at any time t and at equilibrium, respectively, d (cm) is the diameter of the adsorbent, and D (cm^2/min) is the intraparticle diffusion coefficient.

2-4. Validity of the Kinetic Model

The validity of the kinetic model is verified by normalized standard deviation, Δq(%), and can be expressed as Eq. (5) [20].

$$\Delta q(\%) = 100 \times \sqrt{\frac{\Sigma[(q_{exp} - q_{cal})/q_{exp}]^2}{N-1}} \quad (5)$$

where N is the number of data points and q_{exp} and q_{cal} (mg/g) are the experimental and calculated adsorption capacity, respectively.

3. Paclitaxel Analysis

To analyze the content of paclitaxel, an HPLC system (SCL-10AVP, Shimadzu, Japan) and a Capcell Pak C18 column (250×4.6 mm, Shiseido, Japan) were used. The mobile phase was an acetonitrile-water mixture (35/65-65/35, v/v, gradient mode) and the flow rate was 1.0 mL/min. The injection volume was 20 μL and was detected by UV at 227 nm [21]. Authentic paclitaxel (purity: 95%) was purchased from Sigma-Aldrich and was used as a standard.

RESULTS AND DISCUSSION

1. Adsorption Using Cavitation Bubble and Gas Bubble

In this study, an improved adsorption method is proposed for the separation and purification of paclitaxel that can reduce intraparticle diffusion resistance and increase adsorbed amount. In the case of the control group (conventional adsorption; Fig. 2), the adsorbed amount of paclitaxel increased as the adsorption time elapsed, and the maximum adsorbed amount was 300 mg/g (adsorption 10 min). In the case of the ultrasonic cavitation bubble-adsorption with mixing (Fig. 2), the change in the adsorbed amount at the adsorption times of 1, 4, 7, and 10 min was, respectively, 374.452, 375.493, 378.416, and 381.964 mg/g (80 W); 402.516, 404.999, 405.114, and 407.985 mg/g (180 W); and 426.375, 427.416, 430.155, and 431.515 mg/g (250 W). Unlike the control group, there was almost no change in the adsorbed amount in accordance with adsorption time, which indicates that adsorption was completed

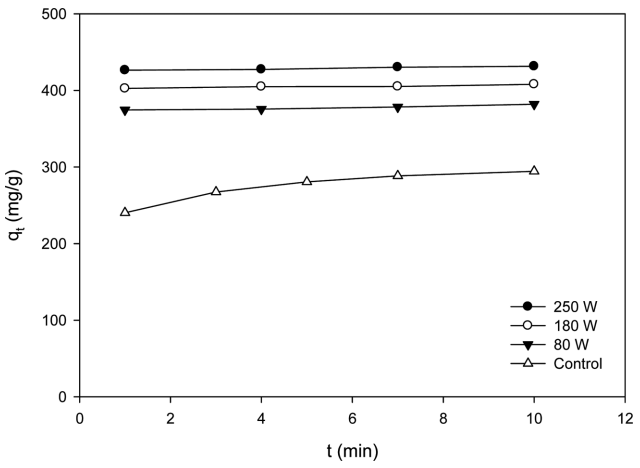

Fig. 2. Adsorption kinetics of paclitaxel onto Sylopute with mixing (~180 rpm) at different ultrasonic powers (paclitaxel concentration: 6,500 mg/L, Sylopute/solution: 10 g/L).

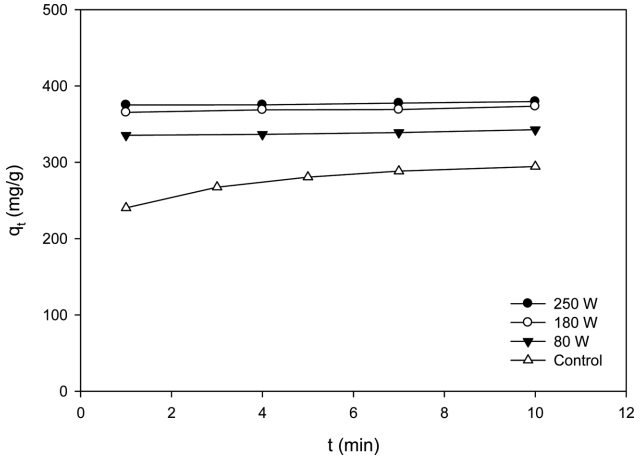

Fig. 3. Adsorption kinetics of paclitaxel onto Sylopute without mixing at different ultrasonic powers (paclitaxel concentration: 6,500 mg/L, Sylopute/solution: 10 g/L).

rapidly in the initial period (~1 min). As the ultrasonic power increased, the adsorbed amount also increased. The maximum adsorbed amount increased 1.27 times (80 W), 1.36 times (180 W), and 1.44 times (250 W) compared with the control group, which shows that the increase rate was higher as the ultrasonic power increased. In the existing literature, cases can be found for both the adsorbed amount increasing and the adsorbed amount decreasing as the ultrasonic power increases in ultrasonic adsorption [10, 11], and this result corresponds to the former. In general, the increase or decrease of the adsorbed amount is explained by improved mass transfer [11] and weakened adsorbent-adsorbate affinity [10] due to high-speed microjects and high-pressure shock waves caused by acoustic cavitation.

To investigate the effect of mixing, the change of adsorbed amount in accordance with adsorption time in ultrasonic cavitation bubble-adsorption without mixing was determined (Fig. 3). At adsorption time of 1, 4, 7, and 10 min, the adsorbed amount was, respectively, 335.417, 336.542, 338.975, and 342.615 mg/g (80 W); 365.416, 368.650, 369.072, and 373.416 mg/g (180 W); and 375.115, 375.214, 377.503, and 379.517 mg/g (250 W). As in the case of mixing, the adsorbed amount was almost unchanged with different adsorption time, indicating that adsorption was quickly completed in the initial period (~1 min). The maximum adsorbed amount increased 1.14 times (80 W), 1.24 times (180 W), and 1.27 times (250 W) compared with the control group, showing that the increase rate became higher as ultrasonic power increased. In addition, compared with the case of mixing, the maximum adsorbed amount decreased by only about 10% (80 W), 8% (180 W), and 12% (250 W). From these results, it was found that the increase in adsorbed amount was more affected by ultrasonic waves than by mixing. This is consistent with previous studies that show that the adsorption rate is much more dependent on ultrasonic waves than on simple stirring [10].

Next, an adsorption experiment was performed by introducing a gas bubble instead of an ultrasonic cavitation bubble under the same adsorption conditions. That is, an adsorption experiment without mixing was performed while changing the gas flow rate to

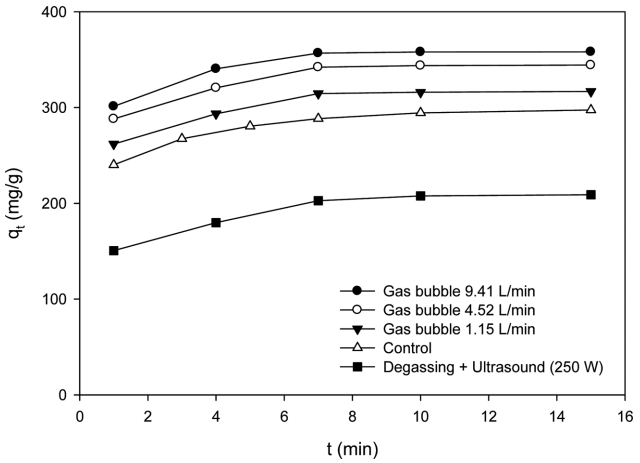

Fig. 4. Adsorption kinetics of paclitaxel onto Sylopute using gas bubble at different gas flow rates and degassed solution without mixing at an ultrasonic power of 250 W (paclitaxel concentration: 6,500 mg/L, Sylopute/solution: 10 g/L).

1.15, 4.52, and 9.41 L/min through a gassing unit. The adsorbed amount at adsorption times of 1, 4, 7, 10, and 15 min (Fig. 4) was, respectively, 261.926, 293.416, 314.515, 315.999, and 316.784 mg/g (1.15 L/min); 288.071, 320.488, 342.146, 343.689, and 344.285 mg/g (4.52 L/min); and 301.227, 340.416, 356.749, 358.000, and 358.146 mg/g (9.41 L/min). Compared with the control, the maximum adsorbed amount increased by 1.06 times (1.15 L/min), 1.15 times (4.52 L/min), and 1.19 times (9.41 L/min), showing that the increase rate was higher as the gas flow rate increased. However, the maximum adsorbed amount decreased by 5.6-16.5% compared with the ultrasonic cavitation bubble-adsorption without mixing. To determine the role of the bubble in the adsorption process, ultrasonic adsorption (ultrasonic power: 250 W) without mixing was performed using a degassed solution (i.e., no cavitation). The adsorbed amounts were 150.518, 179.874, 202.740, 207.695, and 208.914 mg/g at adsorption times of 1, 4, 7, 10, and 15 min, respectively (Fig. 4). The maximum adsorbed amount was reduced by 30% compared with the control group and 45% compared with ultrasonic adsorption without mixing (ultrasonic power: 250 W, no degassing). From these results, it was found that cavitation (bubble) is a critical factor in increasing the adsorbed amount.

2. Analysis of Adsorption Kinetics Using Pseudo-second-order Model

The batch experimental data of the control, ultrasonic adsorption with mixing, ultrasonic adsorption without mixing, ultrasonic adsorption using degassed solution (no mixing), and adsorption using gas bubbles were applied to the pseudo-second-order kinetic model, and t/q_t vs. t was plotted (data not shown). The parameters calculated based on the slope and intercept are shown in Table 1 and Table 2. In the case of the control group (Table 1), the adsorption rate constant k_2 was 0.0091 g/mg·min. Meanwhile, in the case of ultrasonic adsorption with mixing (Table 1), the rate constant k_2 was 0.0676, 0.0823, and 0.0882 g/mg·min at ultrasonic power of 80, 180, and 250 W, respectively. As the ultrasonic power increased, the rate constant k_2 increased. Compared with the control, the rate constant increased by 7.44 times (80 W), 9.06 times (180 W), and 9.71 times (250 W). As the ultrasonic power increased, the increase rate was higher accordingly. In the case of ultrasonic adsorption without mixing (Table 1), the rate constant k_2 at 80, 180, and 250 W of ultrasonic power was 0.0421, 0.0729,

Table 1. Parameters of pseudo-second-order kinetic model for ultrasonic adsorption of paclitaxel

Adsorption type	Ultrasonic power (W)	$q_{e,exp}$ (mg/g)	Pseudo-second-order kinetic model			
			$q_{e,cal}$ (mg/g)	k_2 (g/mg·min)	r^2	Δq (%)
Control	-	303.030	295.858	0.0091	0.9999	3.41
Ultrasonic adsorption with mixing	80	384.615	383.142	0.0676	0.9999	0.96
	180	416.667	415.455	0.0823	1.0000	1.68
	250	434.783	433.651	0.0882	0.9999	0.67
Ultrasonic adsorption without mixing	80	344.828	342.466	0.0421	0.9999	1.77
	180	370.370	369.004	0.0729	0.9999	1.16
	250	384.615	383.436	0.0845	1.0000	1.13
Ultrasonic adsorption using a degassed solution (without mixing)	250	217.391	209.497	0.0081	0.9991	4.38

Table 2. Parameters of pseudo-second-order kinetic model for gas bubble-adsorption of paclitaxel

Adsorption type	Gas flow rate (L/min)	$q_{e,exp}$ (mg/g)	Pseudo-second-order kinetic model			
			$q_{e,cal}$ (mg/g)	k_2 (g/mg·min)	r^2	Δq (%)
Gas bubble-adsorption	1.15	322.581	316.456	0.0107	0.9998	2.45
	4.52	357.143	351.288	0.0112	0.9998	2.50
	9.41	370.370	364.964	0.0122	0.9999	1.75

and 0.0845 g/mg·min, respectively. As the ultrasonic power increased, the rate constant k_2 increased. Compared with the control, the rate constant increased by 4.63 times (80 W), 8.03 times (180 W), and 9.31 times (250 W), which shows that the increase rate was higher as the ultrasonic power increased. In addition, the adsorption rate constant decreased by 38, 11, and 4%, respectively, compared with the ultrasonic adsorption with mixing. In the absence of mixing, the rate constant decreased even more as the ultrasonic power decreased. This is because, in the absence of mixing, ultrasound greatly contributed to mass transfer in the pores of the adsorbent as well as mixing [11,12]. In the case of ultrasonic adsorption using degassed solution (Table 1), the rate constant k_2 was 0.0081 g/mg·min, which is 10% lower than that of the control, indicating that cavitation (bubble) is an important factor in increasing the rate constant [22, 23]. In the case of adsorption using gas bubbles (Table 2), the rate constant k_2 was 0.0107, 0.0112, and 0.0122 g/mg·min at gas flow rates of 1.15, 4.52 and 9.41 L/min, respectively, which shows that the rate constant increased as the gas flow rate increased. Compared with the control, the rate constant increased by 1.18 times (1.15 L/min), 1.23 times (4.52 L/min), and 1.34 times (9.41 L/min), which shows that the rate constant slightly increased as the flow rate increased. However, the rate constant decreased by 74.6-85.6% compared with the adsorption using cavitation bubble (no mixing). From these results, it was found that the cavitation bubble had a greater effect on the adsorption rate constant than the gas bubble. The higher r^2 values (>0.9991) and the lower Δq (%) values (<4.38) revealed that the second-order kinetic model was suitable. The calculated $q_{e,cal}$ values also agreed well with the experimental data ($q_{e,exp}$).

3. Analysis of Adsorption Kinetics Using Intraparticle Diffusion Model

In general, the plot of q_t versus $t^{1/2}$ by the intraparticle diffusion model is multi-linear and there are three different portions. The first portion is a step in which the adsorbate moves through the solution to the outer surface of adsorbent (boundary layer diffusion), the second portion is a step in which the adsorbate diffuses into the pores of the adsorbent (intraparticle diffusion), and the third portion is a step in which the adsorbate is adsorbed on the sites of the inner surface of the adsorbent to reach equilibrium (final equilibrium) [24,25]. The batch experimental data of the control, ultrasonic adsorption with mixing, ultrasonic adsorption without mixing, ultrasonic adsorption using degassed solution (no mixing), and adsorption using gas bubbles were applied to the intraparticle diffusion model, and q_t vs. $t^{1/2}$ was plotted (Fig. 5). In the

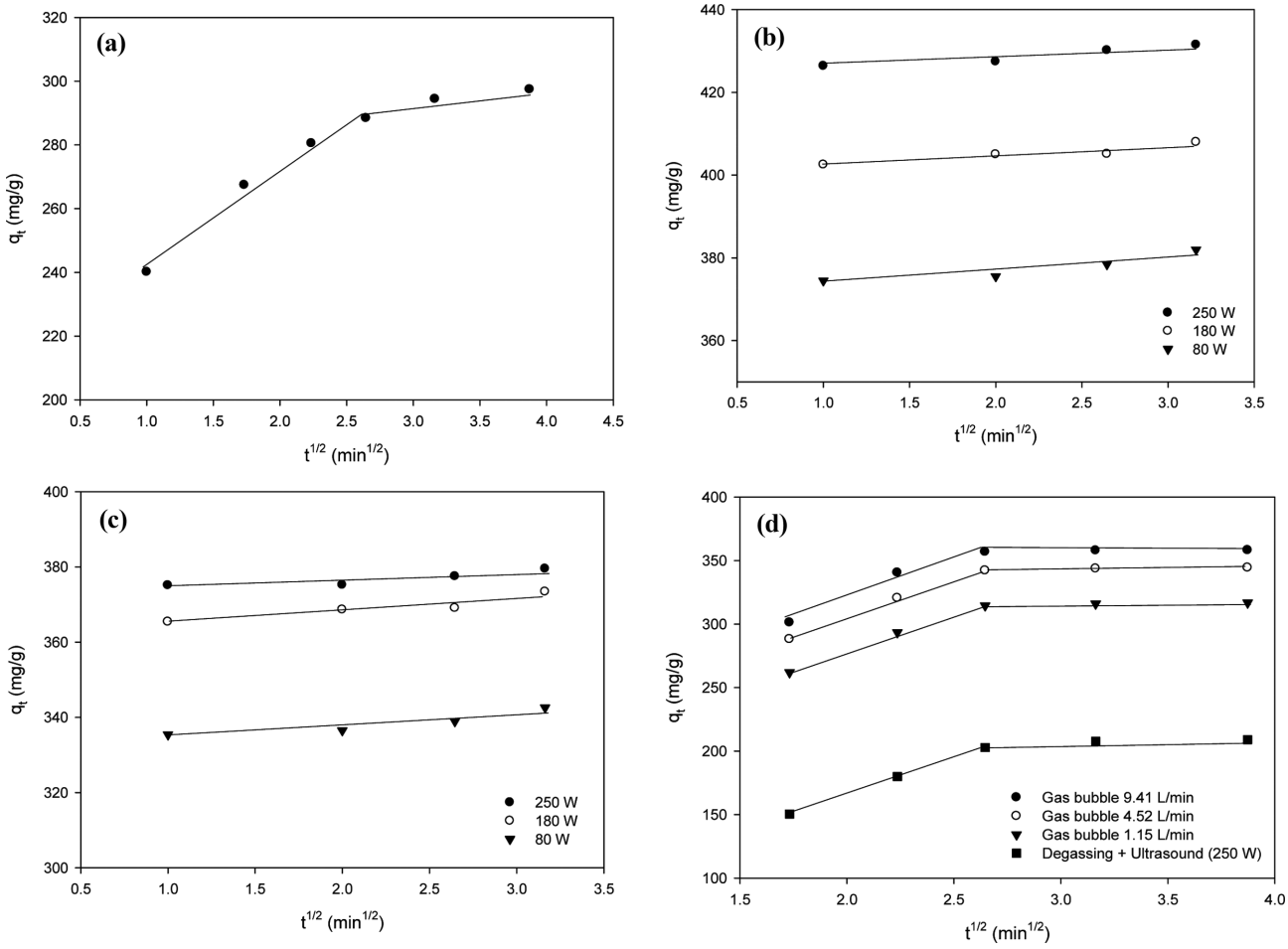

Fig. 5. Intraparticle diffusion model for conventional adsorption (a), ultrasound-assisted adsorption with mixing (~180 rpm) (b), ultrasound-assisted adsorption without mixing (c), and adsorption of paclitaxel using gas bubble and degassed solution (d).

case of the control (Fig. 5(a)), adsorption using gas bubbles, and ultrasonic adsorption (no mixing) using a degassed solution (Fig. 5(d)), the intraparticle diffusion and equilibrium steps were observed. In the case of ultrasonic adsorption (Fig. 5(b) and Fig. 5(c)), only the equilibrium step was observed. Thus, in the case of the control, adsorption using gas bubbles, and ultrasonic adsorption (no mixing) using a degassed solution, intraparticle diffusion was confirmed as a rate-limiting step; whereas, in the case of ultrasonic adsorption, it was found that adsorption was achieved without the resistance of boundary layer diffusion (film diffusion, external mass transfer) and intraparticle diffusion (mass transfer through the pores). Consequently, it was difficult to eliminate the effect of intraparticle diffusion resistance by adsorption using gas bubbles and ultrasonic adsorption using a degassed solution (without a cavitation bubble). In addition, irrespective of mixing or not, by introducing ultrasound into the adsorption process, the rate-limiting step could be effectively eliminated by reducing the intraparticle diffusion resistance. Ultrasound thus played a key role, rather than mixing, in eliminating the rate-limiting step because of intraparticle diffusion resistance in the adsorption process. In the case of ultrasonic adsorption, shock waves/microjets caused by collapse of the cavitation bubble, rather than the bubble itself, are considered as promoting mass transfer within the pores of the adsorbent (Fig. 6) [10,26]. This is consistent with the results of previous studies that showed that, when the rate-limiting step is boundary layer diffusion (film diffusion, external mass transfer), mixing has a greater effect on adsorption, and, when the rate-limiting step is intraparticle diffusion (mass transfer through the pores), ultrasound has a greater effect on adsorption [11,12]. On the other hand, unlike the cavitation bubble, the gas bubble just expands and does not collapse, so shock waves, microjets, and high temperature/high pressure do not occur [27]. As a result, in the case of ultrasonic adsorption, the cavitation bubble increases the adsorbed amount and also promotes intraparticle diffusion, thereby eliminating the rate-limiting step. In contrast, in the case of the gas bubble, it is possible to increase the adsorbed amount to some extent, but there is a limit to promoting intraparticle diffusion. In particular, in adsorption using a degassed solution, no ultrasonic cavitation bubble was observed (data not shown), and for this reason there was no improvement of intraparticle diffusion resistance. In addition, the parameters calculated using the intraparticle diffusion model in the control, gas bubble-adsorption, and ultrasonic adsorption using a degassed solution,

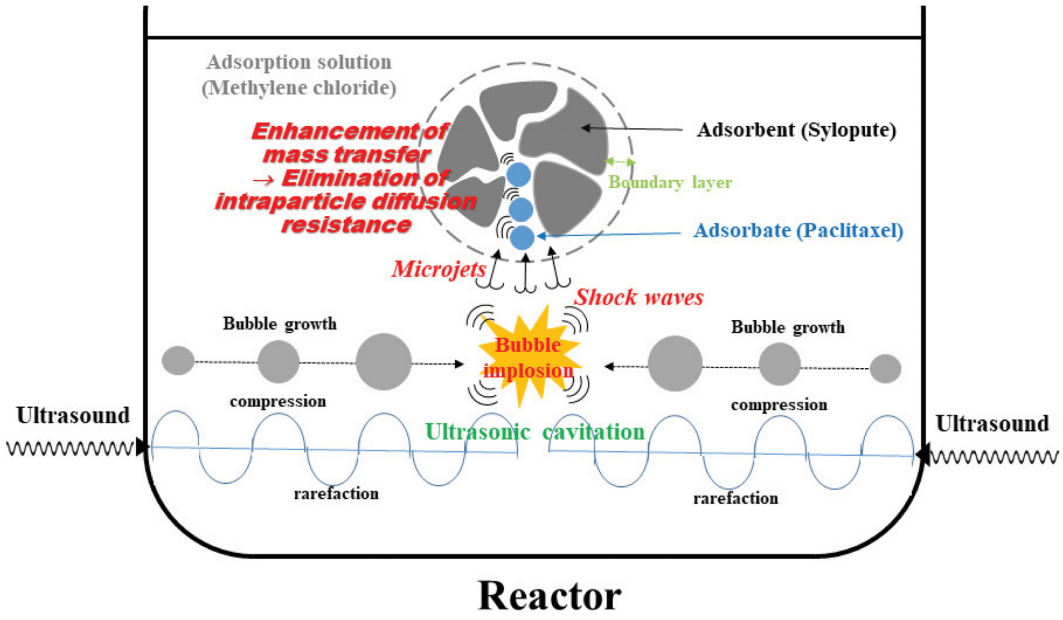

Fig. 6. A proposed mechanism for cavitation bubble-induced adsorption of paclitaxel.

Table 3. Parameters of intraparticle diffusion model for adsorption of paclitaxel using gas bubble and degassed solution

Adsorption type	Gas flow rate (L/min)	Intraparticle diffusion model			
		$q_{e,cal}$ (mg/g)	k_p (mg/g·min$^{1/2}$)	r^2	Δq (%)
Control	-	327.362	29.5720	0.9808	4.93
Gas bubble-adsorption	1.15	353.496	31.9150	0.9999	5.59
	4.52	382.251	32.8200	0.9999	5.32
	9.41	400.905	34.2050	0.9880	5.85
Ultrasonic adsorption using a degassed solution (without mixing)	-	231.492	27.7000	0.9773	5.07

Table 4. Intraparticle diffusion coefficients for adsorption of paclitaxel using gas bubble and degassed solution

Adsorption type	Gas flow rate (L/min)	Intraparticle diffusion coefficient, D (cm^2/min)	r^2
Control	-	2.3225×10^{-15}	0.9945
Gas bubble-adsorption	1.15	3.1171×10^{-15}	0.9654
	4.52	3.3271×10^{-15}	0.9680
	9.41	4.0736×10^{-15}	0.9852
Ultrasonic adsorption using a degassed solution (without mixing)	-	2.2278×10^{-15}	0.9670

excluding ultrasonic adsorption without intraparticle diffusion resistance, are shown in Table 3. The intraparticle diffusion rate constant was 29.5720 mg/g·$min^{1/2}$ in the case of the control; 31.9150 mg/g·$min^{1/2}$ (1.15 L/min), 32.8200 mg/g·$min^{1/2}$ (4.52 L/min), and 34.2050 mg/g·$min^{1/2}$ (9.41 L/min) in the case of adsorption using gas bubble; and 27.7000 mg/g·$min^{1/2}$ in the case of ultrasonic adsorption using a degassed solution. Compared with the control, the intraparticle diffusion rate constant increased 8% (1.15 L/min), 11% (4.52 L/min), and 16% (9.41 L/min) in adsorption using gas bubble. As the gas flow rate increased, the intraparticle diffusion rate increased accordingly. Adsorption using a degassed solution decreased by 6% compared with the control. Further, in order to calculate the intraparticle diffusion coefficient, $-\log[1-(q/q_e)^2]$ vs. t was plotted (data not shown). The intraparticle diffusion coefficient calculated based on the slope in Eq. (3) is presented in Table 4 and was 2.3225×10^{-15} cm^2/min for the control and 3.1171×10^{-15} (1.15 L/min), 3.3271×10^{-15} (4.52 L/min), and 4.0736×10^{-15} cm^2/min (9.41 L/min) for adsorption using gas bubble. Compared with the control, the intraparticle diffusion coefficient increased by 1.34 times (1.15 L/min), 1.43 times (4.52 L/min), and 1.75 times (9.41 L/min), showing that the intraparticle diffusion coefficient increased as the gas flow rate increased. These results are similar to a study in which the intraparticle diffusion coefficient increased by 1.5-1.7 times compared with the control (conventional method) in ultrasonic adsorption (adsorbent: dead pine needles, 40 kHz ultrasonic bath, power 125 W) for the removal of malachite green [19]. From this, it is thought that gas bubbles also contributed to some extent in improving mass transfer in the pores of the adsorbent [28]. In the ultrasonic adsorption using a degassed solution, the intraparticle diffusion coefficient was 2.2278×10^{-15} cm^2/min, which was 4% lower than that of the control and confirms that the cavitation bubble had a decisive influence on the intraparticle diffusion coefficient.

CONCLUSIONS

A novel paclitaxel adsorption method has been proposed that can increase the adsorbed amount as well as promote intraparticle diffusion. Conventional adsorption (control), ultrasonic adsorption with mixing, ultrasonic adsorption without mixing, ultrasonic adsorption with degassed solution (no mixing), and gas bubble-adsorption were performed. Compared with the control, the maximum adsorbed amount and adsorption rate constant increased, respectively, by 1.27-1.44 times and 7.44-9.71 times (ultrasonic adsorption with mixing at 80-250 W), 1.14-1.27 times and 4.63-9.31 times (ultrasonic adsorption without mixing at 80-250 W), and 1.06-1.19 times and 1.18-1.34 times (gas bubble-adsorption at 1.15-9.41 L/min). On the other hand, in the case of ultrasonic adsorption (no mixing) using a degassed solution (i.e., no cavitation), the maximum adsorbed amount and adsorption rate constant decreased by 30% and 10%, respectively, compared with the control. The presence or absence of ultrasound had a greater effect on the increase in the adsorbed amount than the presence or absence of mixing. The adsorption rate constant of ultrasonic adsorption without mixing was reduced by about 4-38% compared with ultrasonic adsorption with mixing. In the absence of mixing, because ultrasound contributes to mixing and mass transfer in the pores of the adsorbent, the adsorption rate constant decreased more as the ultrasound power decreased. From the analysis of adsorption kinetics using the intraparticle diffusion model, diffusion within the particles was promoted sufficiently because of efficient mass transport in the pores of the adsorbent by microjets and shock waves generated by bubble collapse rather than the cavitation bubble itself. On the other hand, in the case of gas bubbles, although the intraparticle diffusion coefficient increased by 1.34-1.75 times compared with the control, there was a limit to the promotion of intraparticle diffusion. The results show that ultrasonic adsorption can increase the adsorbed amount and also improve the diffusion resistance within the particles efficiently. In contrast, although gas bubble-adsorption can increase the adsorbed amount, there is a limit to the improvement of the diffusion resistance within the particles.

ACKNOWLEDGEMENTS

This work was supported by the National Research Foundation of Korea (NRF) grant funded by the Korea government (MSIT) (Grant Number: 2021R1A2C1003186).

REFERENCES

1. H. J. Kang and J. H. Kim, *Biotechnol. Bioprocess Eng.*, **25**, 86 (2020).
2. A. M. L. Seca and D. C. G. A. Pinto, *Int. J. Mol. Sci.*, **19**, 263 (2018).
3. H. J. Kang and J. H. Kim, *Korean J. Chem. Eng.*, **36**, 1965 (2019).
4. S. H. Pyo, H. J. Choi and B. H. Han, *J. Chromatogr. A*, **1123**, 15 (2006).
5. H. W. Seo and J. H. Kim, *Process Biochem.*, **87**, 238 (2019).
6. S. H. Pyo, H. B. Park, B. K. Song, B. H. Han and J. H. Kim, *Process Biochem.*, **39**, 1985 (2004).
7. K. W. Yoo and J. H. Kim, *Biotechnol. Bioprocess Eng.*, **23**, 532 (2018).

8. C. G. Lee and J. H. Kim, *Korean Chem. Eng. Res.*, **54**, 89 (2016).
9. Y. S. Lim and J. H. Kim, *J. Chem. Thermodyn.*, **115**, 261 (2017).
10. O. Hamdaoui, E. Naffrechoux, L. Tifouti and C. Pétrier, *Ultrson. Sonochem.*, **10**, 109 (2003).
11. O. Hamdaoui and E. Naffrechoux, *Ultrson. Sonochem.*, **16**, 15 (2009).
12. B. S. Schueller and R. T. Yang, *Ind. Eng. Chem. Res.*, **40**, 4912 (2001).
13. X. Zhou, G. Jing, B. Lv, Z. Zhou and R. Zhu, *Chemosphere*, **160**, 332 (2016).
14. J. Y. Lee and J. H. Kim, *Sep. Purif. Technol.*, **103**, 8 (2013).
15. H. S. Kim and J. H. Kim, *Process Biochem.*, **56**, 163 (2017).
16. P. Maneechakr and S. Karnjanakom, *J. Chem. Thermodyn.*, **106**, 104 (2017).
17. D. N. Cho and J. H. Kim, *Korean Chem. Eng. Res.*, **58**, 127 (2020).
18. S. H. Park and J. H. Kim, *Korean Chem. Eng. Res.*, **58**, 113 (2020).
19. O. Hamdaoui, M. Chiha and E. Naffrechoux, *Ultrson. Sonochem.*, **15**, 799 (2008).
20. F. C. Wu, R. L. Tseng and R. S. Juang, *J. Colloid Interface Sci.*, **283**, 49 (2005).
21. Y. S. Kim and J. H. Kim, *J. Chem. Thermodyn.*, **130**, 104 (2019).
22. M. Ondarts, L. Reinert, S. Guittonneau, S. Baup, S. Delpeux, J. M. Lévêque and L. Duclaux, *Chem. Eng. J.*, **343**, 163 (2018).
23. J. B. Ji, X. H. Lu and Z. C. Xu, *Ultrson. Sonochem.*, **13**, 463 (2006).
24. H. J. Kang and J. H. Kim, *Biotechnol. Bioprocess Eng.*, **24**, 513 (2019).
25. H. S. Shin and J. H. Kim, *Process Biochem.*, **51**, 917 (2016).
26. L. Wolloch and J. Kost, *J. Control. Release*, **148**, 204 (2010).
27. K. Wohlgemuth, A. Kordylla, F. Ruether and G. Schembecker, *Chem. Eng. Sci.*, **64**, 4155 (2009).
28. R. Krishna, J. Ellenberger, M. I. Urseanu and F. J. Keil, *Naturwissenschaften*, **87**, 455 (2000).